

## Mn 2*p* core-level spectra of La<sub>1-x</sub>Ba<sub>x</sub>MnO<sub>3</sub> thin films using hard x-ray photoelectron spectroscopy: Relation between electronic and magnetic states

S. Ueda,<sup>1</sup> H. Tanaka,<sup>2</sup> E. Ikenaga,<sup>3</sup> J. J. Kim,<sup>3</sup> T. Ishikawa,<sup>4</sup> T. Kawai,<sup>2</sup> and K. Kobayashi<sup>1</sup>

<sup>1</sup>*NIMS Beamline Station at SPring-8, National Institute for Materials Science, Sayo, Hyogo 678-5148, Japan*

<sup>2</sup>*Institute of Scientific and Industrial Research, Osaka University, Ibaraki, Osaka 567-0047, Japan*

<sup>3</sup>*Japan Synchrotron Radiation Research Institute (JASRI), SPring-8, Sayo, Hyogo 678-5198, Japan*

<sup>4</sup>*RIKEN, SPring-8, Sayo, Hyogo 678-5148, Japan*

(Received 13 April 2009; revised manuscript received 12 August 2009; published 8 September 2009)

We have measured the Mn 2*p* core-level hard x-ray photoelectron spectra for La<sub>0.85</sub>Ba<sub>0.15</sub>MnO<sub>3</sub> thin films to investigate the temperature dependence on electronic and magnetic states. We can explain the relation between the Mn 2*p* core-level spectra and magnetization for La<sub>0.85</sub>Ba<sub>0.15</sub>MnO<sub>3</sub> using the *t*-*J* model and the Bloch  $T^{3/2}$  law under the assumption that the Hund coupling between the Mn *e<sub>g</sub>* and *t<sub>2g</sub>* states is strong enough. This result means that the magnon excitation plays an important role in physical properties of manganites.

DOI: [10.1103/PhysRevB.80.092402](https://doi.org/10.1103/PhysRevB.80.092402)

PACS number(s): 75.30.Et, 75.70.-i, 79.60.-i, 78.70.Dm

Research fields of spintronics have been expanded for further electronic device applications utilizing spin degree of freedom. One of the potential materials for spintronics is perovskite manganites, because manganites show a rich variety of physical properties such as colossal magnetoresistance,<sup>1</sup> ferromagnetism with metallic conduction,<sup>2</sup> and perfect spin polarization.<sup>3</sup> To understand their physical properties, the experimental methods, which probe intrinsic electronic states of solid, are needed.

Hard x-ray photoelectron spectroscopy (HX-PES) is a powerful tool to investigate electronic structures of solids without careful surface cleaning in many cases due to a large probing depth of high kinetic energy photoelectrons.<sup>4</sup> Using an advantage of the large probing depth in HX-PES experiments, Horiba *et al.*<sup>5</sup> reported that the Mn 2*p* core-level HX-PES revealed the intrinsic electronic states of La<sub>1-x</sub>Sr<sub>x</sub>MnO<sub>3</sub> (LSMO) thin films. In their work, for comparison the HX-PES with soft x-ray PES, an additional well-screened structure was only observed in the Mn 2*p* core-level HX-PES spectra. Tanaka *et al.*<sup>6</sup> reported the temperature dependence of the Mn 2*p* core-level HX-PES spectra for the La<sub>0.85</sub>Ba<sub>0.15</sub>MnO<sub>3</sub> (LBMO) thin film, and showed that the intensity of the well-screened structure (*I<sub>s</sub>*) increased with decreasing temperature. The well-screened structure in the Mn 2*p* HX-PES spectra cannot reproduced by the MnO<sub>6</sub> cluster model calculation based on the configuration interaction, but the model with an additional hybridization term (*V\**), which is the hybridization strength between the Mn 3*d* states and coherent states at the Fermi level,<sup>5-8</sup> represents the Mn 2*p* HX-PES spectral features in LBMO and LSMO. It is considered that the mechanism of the ferromagnetic metal state in perovskite manganites arises from a carrier-mediated ferromagnetism through the double exchange interaction.<sup>9</sup> By comparing the HX-PES spectra of LBMO with the carrier mediated ferromagnetism, Tanaka *et al.* proposed that *I<sub>s</sub>* was proportional to the square of the magnetization (*M*). They also experimentally showed that *I<sub>s</sub>* was proportional to the square of *V\**. However the relation between the HX-PES spectra and magnetism in the perovskite manganites is an issue to be solved.

In this Brief Report, we report the temperature depen-

dence on the Mn 2*p* core-level spectra for LBMO thin films and discuss the relation between the electronic and magnetic states to understand the physical properties of perovskite manganites in the ferromagnetic metal phase.

5-nm-thick La<sub>0.85</sub>Ba<sub>0.15</sub>MnO<sub>3</sub> epitaxial thin film was deposited on etched 0.01 wt% Nb-doped SrTiO<sub>3</sub> (001) substrates using a pulsed laser deposition technique. The detail sample preparation was described elsewhere.<sup>10,11</sup> The temperature dependence on magnetization was measured using a superconducting quantum interference device (SQUID). Curie temperature (*T<sub>C</sub>*) of the film was found to be about 220 K. The electrical resistivity was measured using a four-probe method. The Mn 2*p* core-level HX-PES measurements were performed at the undulator beamline BL29XU of SPring-8. The experimental setup was described elsewhere.<sup>4,12</sup> The excitation photon energy was set to 7.94 keV. Total-energy resolution was set to 250 meV, which was evaluated from the Fermi cutoff of a Au foil.

Figure 1 shows the Mn 2*p* core-level HX-PES spectra for the 5-nm-thick LBMO film measured at various temperatures. The Mn 2*p* spectra consist of the main (~642 eV) and satellite (~639.5 eV) structures. *I<sub>s</sub>* decreased with increasing temperature, while the spectral shape of the main structure did not show remarkable change in the entire temperature range. At above *T<sub>C</sub>*, *I<sub>s</sub>* was very weak. These tendencies were observed in the previous work for the 20-nm-thick LBMO film.<sup>6</sup> By comparing the Mn 2*p* spectral shapes of the 5-nm-thick LBMO film with those of the 20-nm-thick LBMO film, *I<sub>s</sub>* for the 5 nm-thick LBMO film is found to be weaker than that for the 20-nm-thick LBMO film at low temperature. This result seemed that *I<sub>s</sub>* related to the strength of ferromagnetic interaction in LBMO. We evaluated the value of *V\** at various temperatures by comparing the Mn 2*p* core-level spectral shapes of the 5-nm-thick LBMO with those of the 20-nm-thick LBMO film. The evaluated *V\** was shown in Table I. As seen in the case of the 20-nm-thick LBMO film,<sup>6</sup> we see that *V\** of the 5-nm-thick LBMO film is also a temperature-dependent parameter.

Let us consider how the Mn 2*p* spectral change relates to *M*, while *I<sub>s</sub>* was found to be almost proportional to *M*<sup>2</sup> as reported in Ref. 6. To reduce *M* from the Mn 2*p* HX-PES

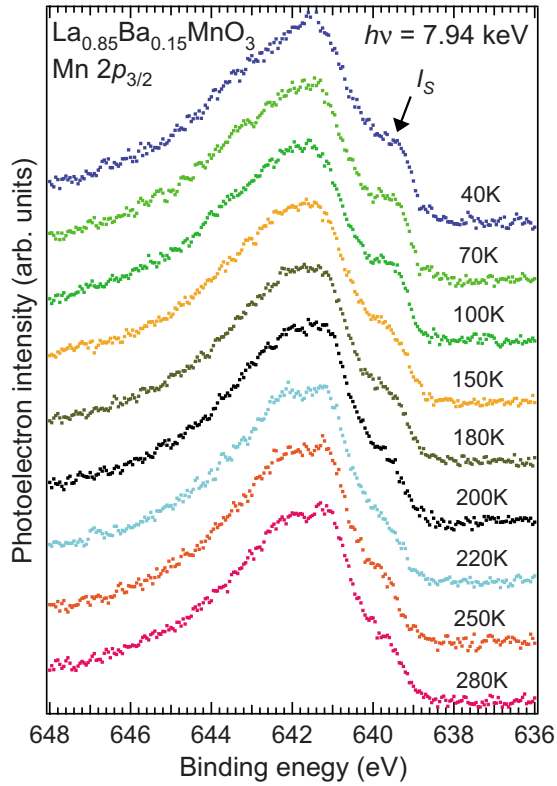


FIG. 1. (Color online) Mn  $2p$  core-level spectra for the 5-nm-thick  $\text{La}_{0.85}\text{Ba}_{0.15}\text{MnO}_3$  film measured at various temperatures.

spectra, first one needs to consider how the exchange interaction ( $J$ ) in LBMO can be explained. It is known that the ferromagnetic metal in the perovskite manganites is represented by the double exchange model,<sup>9</sup> in which the transfer integral ( $t$ ) between the Mn  $e_g$  sites and the Hund coupling ( $J_H$ ) between the Mn  $e_g$  and  $t_{2g}$  states are considered. Under the assumption that  $J_H$  was strong enough between the Mn  $e_g$  and  $t_{2g}$  states, the double exchange model should be simplified to the  $t$ - $J$  model.<sup>13</sup> In the model,  $J$  is proportional to  $t^2/U$ , where  $U$  is the Mn  $3d$ - $3d$  Coulomb interaction. When we consider that  $V^*$  qualitatively represents the Mn  $3d$ - $3d$  transfer integral, one get that  $t$  is proportional to  $V^*$ , leading that  $J$  is proportional to the square of  $V^*$ . As  $J$  is the ferromagnetic exchange interaction in the above situation, the relation between  $M$  and  $J$  can be represented by using the

TABLE I. Electronic structure parameter  $V^*$  for the 5-nm-thick LBMO thin film at various temperatures. The value of  $V^*$  was evaluated by comparing the present results with the previous work (Ref. 6).

Temperature (K)	$V^*$ (eV)	Temperature (K)	$V^*$ (eV)
40	0.33	200	0.29
70	0.33	220	0.24
100	0.32	250	0.24
150	0.29	280	0.24
180	0.29		

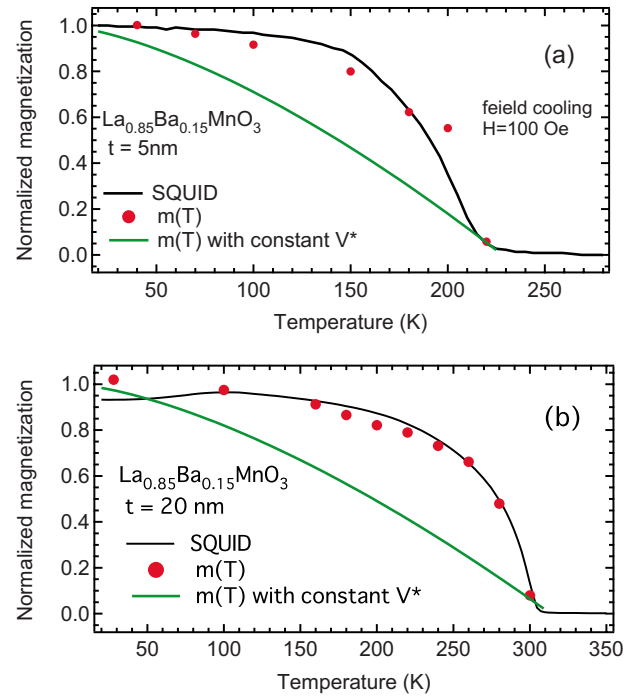


FIG. 2. (Color online) Normalized magnetization curves for the  $\text{La}_{0.85}\text{Ba}_{0.15}\text{MnO}_3$  films with thickness of (a) 5 and (b) 20 nm measured by SQUID magnetometer. The calculated  $m(T)$  curves using Eq. (1) were also shown in the figure.

Bloch  $T^{3/2}$  law.<sup>14</sup> Then the temperature-dependent normalized magnetization,  $m(T)$ , is given as follows:

$$m(T) = 1 - A[k_B T / (V^*)^2]^{3/2}, \quad (1)$$

where  $A$  is a coefficient and  $k_B$  is Boltzmann constant. We note that  $V^*$  is a temperature-dependent parameter. Figure 2(a) shows the normalized magnetization curve for the 5-nm-thick LBMO film obtained by SQUID and calculated  $m(T)$  using Eq. (1) below  $T_C$ . Calculated  $m(T)$  for the 5-nm-thick LBMO film well reproduces the magnetization curve as well as that for the 20-nm-thick LBMO film as shown in Fig. 2(b). These results suggest that the magnetism of LBMO in the ferromagnetic metal phase is governed by  $(V^*)^2$ . The density of states at  $E_F[D(E_F)]$  is proportional to  $(V^*)^2$  on the basis of the impurity Anderson model as described in Refs. 5 and 6, thus we can conclude that the ferromagnetic metal phase in the manganites arises from the conducting carriers, i.e.,  $D(E_F)$ . Although  $J$  is constant in the Bloch  $T^{3/2}$  law for simple ferromagnetic metals,  $J$  for the manganites in the ferromagnetic metal phase is affected by  $D(E_F)$ . We note that  $m(T)$  curves for the 5- and 20-nm-thick LBMO films deviate from the magnetization curves obtained by SQUID magnetometer, when  $V^*$  in Eq. (1) is constant in the entire range below  $T_C$  as shown in Fig. 2. Therefore  $I_s$  of the Mn  $2p$  core-level spectra for LBMO reflects  $D(E_F)$  and magnetic information as a function of temperature.

Second we compared the normalized conductivity with calculated  $m(T)$  for the 5- and 20-nm-thick LBMO films as shown in Fig. 3. The normalized conductivity curves agreed well with calculated  $m(T)$  below  $T_C$ . As mentioned above,

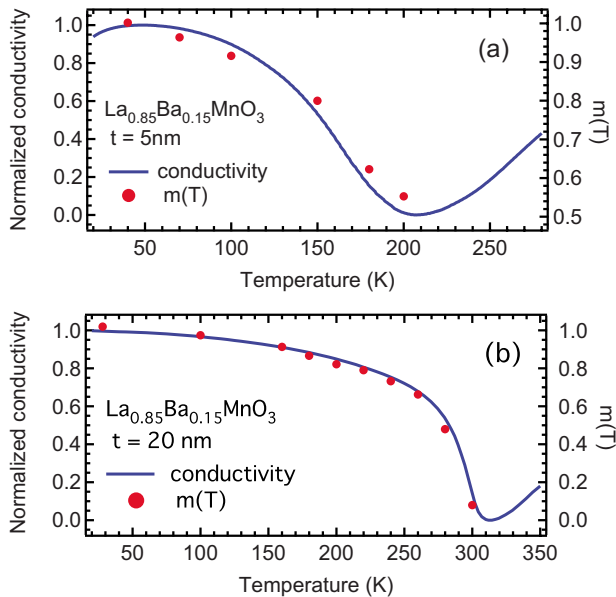


FIG. 3. (Color online) Normalized conductivity curves for the  $\text{La}_{0.85}\text{Ba}_{0.15}\text{MnO}_3$  films with thickness of (a) 5 nm and (b) 20 nm. The calculated  $m(T)$  curves using Eq. (1) was also plotted in the figure.

since Eq. (1) is based on the Bloch  $T^{3/2}$  law, the magnetization decreases with increasing temperature due to the magnon excitations. According to the Anderson-Hasegawa model,<sup>15</sup> the nearest-neighbor Mn  $3d$ - $3d$  transfer integral ( $t$ ) is proportional to  $\cos(\theta/2)$ , where  $\theta$  is the angle between the nearest-neighbor Mn  $3d$  magnetic moments. This means that the magnon excitation decreases  $t$  with increasing temperature. We should note that  $D(E_F)$  for the LBMO film also decreases with increasing temperature as mentioned above. The carrier density for LBMO decreases slowly as temperature increases, while the Hall mobility of LBMO strongly

depends on temperature.<sup>16</sup> The decrease in  $D(E_F)$  has been also reported in the optical conductivity measurement for bulk LSMO in Ref. 17. Although we seem that the behaviors of carriers and magnons as a function of temperature mainly determine the conductivity in Fig. 3, theoretical models are required for collective understanding of the conductivity in the manganites for the ferromagnetic metal.

Finally we considered why  $T_C$  of 5-nm-thick LBMO was suppressed as compared with 20-nm-thick LBMO. The suppression of  $T_C$  can be mainly accounted for by other additional factors such as a surface boundary layer<sup>3,18</sup> and charge transfer between the film and substrate,<sup>19,20</sup> even though the LBMO film was still strained. In fact both  $I_s$  and  $V^*$  for the 5-nm-thick LBMO film decreased in comparison with the 20-nm-thick LBMO film. In addition, the suppression of  $T_C$  and  $I_s$  proceeded in the 3-nm-thick LBMO film as seen in Ref. 6. Therefore the suppression of  $T_C$  in the thin LBMO films mainly originates from carrier modulation effects reflecting the interfacial electronic structure.

In summary, the electronic states of the LBMO thin films were studied by the Mn  $2p$  core-level HX-PES. The magnetization of LBMO was well explained by using the  $t$ - $J$  model and the Bloch  $T^{3/2}$  law through the temperature dependence of the satellite structure measured in the HX-PES spectra. The proposed model interprets the relation between the electronic and magnetic states of the manganites in the ferromagnetic metal case.

The authors would like to thank the staff of BL29XU, RIKEN, and SPring-8, especially Y. Takata, M. Yabashi, K. Tamasaku, and Y. Nishino, for their technical assistance at the beamline. S.U. would like to thank M. Shirai for helpful discussion. The HX-PES measurements were performed under the approval of JASRI/SPring-8 (Proposal No. 2006A1606).

- <sup>1</sup>R. von Helmolt, J. Wecker, B. Holzapfel, L. Schultz, and K. Samwer, Phys. Rev. Lett. **71**, 2331 (1993).
- <sup>2</sup>A. Urushibara, Y. Moritomo, T. Arima, A. Asamitsu, G. Kido, and Y. Tokura, Phys. Rev. B **51**, 14103 (1995).
- <sup>3</sup>J. H. Park, E. Vescovo, H. J. Kim, C. Kwon, R. Ramesh, and T. Venkatesan, Nature (London) **392**, 794 (1998).
- <sup>4</sup>K. Kobayashi, M. Yabashi, Y. Takata, T. Tokushima, S. Shin, K. Tamasaku, D. Miwa, T. Ishikawa, H. Nohira, T. Hattori, Y. Sugita, O. Nakatsuka, A. Sakai, and S. Zaima, Appl. Phys. Lett. **83**, 1005 (2003).
- <sup>5</sup>K. Horiba, M. Taguchi, A. Chainani, Y. Takata, E. Ikenaga, D. Miwa, Y. Nishino, K. Tamasaku, M. Awaji, A. Takeuchi, M. Yabashi, H. Namatame, M. Taniguchi, H. Kumigashira, M. Oshima, M. Lippmaa, M. Kawasaki, H. Koinuma, K. Kobayashi, T. Ishikawa, and S. Shin, Phys. Rev. Lett. **93**, 236401 (2004).
- <sup>6</sup>H. Tanaka, Y. Takata, K. Horiba, M. Taguchi, A. Chainani, S. Shin, D. Miwa, K. Tamasaku, Y. Nishino, T. Ishikawa, E. Ikenaga, M. Awaji, A. Takeuchi, T. Kawai, and K. Kobayashi,

Phys. Rev. B **73**, 094403 (2006).

- <sup>7</sup>M. Taguchi, A. Chainani, K. Horiba, Y. Takata, M. Yabashi, K. Tamasaku, Y. Nishino, D. Miwa, T. Ishikawa, T. Takeuchi, K. Yamamoto, M. Matsunami, S. Shin, T. Yokoya, E. Ikenaga, K. Kobayashi, T. Mochiku, K. Hirata, J. Hori, K. Ishii, F. Nakamura, and T. Suzuki, Phys. Rev. Lett. **95**, 177002 (2005).
- <sup>8</sup>M. Taguchi, A. Chainani, N. Kamakura, K. Horiba, Y. Takata, M. Yabashi, K. Tamasaku, Y. Nishino, D. Miwa, T. Ishikawa, S. Shin, E. Ikenaga, T. Yokoya, K. Kobayashi, T. Mochiku, K. Hirata, and K. Motoya, Phys. Rev. B **71**, 155102 (2005).
- <sup>9</sup>K. Zener, Phys. Rev. **82**, 403 (1951).
- <sup>10</sup>T. Kanki, H. Tanaka, and T. Kawai, Phys. Rev. B **64**, 224418 (2001).
- <sup>11</sup>J. Zhang, H. Tanaka, T. Kanki, J. H. Choi, and T. Kawai, Phys. Rev. B **64**, 184404 (2001).
- <sup>12</sup>Y. Takata, M. Yabashi, K. Tamasaku, Y. Nishino, D. Miwa, T. Ishikawa, E. Ikenaga, K. Horiba, S. Shin, M. Arita, K. Shimada, H. Namatame, M. Taniguchi, H. Nohira, T. Hattori, S. Sodergren, B. Wannberg, and K. Kobayashi, Nucl. Instrum. Methods

- Phys. Res. A **547**, 50 (2005).
- <sup>13</sup>P. W. Anderson, *Science* **235**, 1196 (1987).
- <sup>14</sup>C. Kittel, *Introduction to Solid State Physics*, 6th ed. (John Wiley & Sons, New York, 1986).
- <sup>15</sup>P. W. Anderson and H. Hasegawa, *Phys. Rev.* **100**, 675 (1955).
- <sup>16</sup>T. Kanki, T. Yanagida, B. Vilquin, H. Tanaka, and T. Kawai, *Phys. Rev. B* **71**, 012403 (2005).
- <sup>17</sup>Y. Okimoto, T. Katsufuji, T. Ishikawa, T. Arima, and Y. Tokura, *Phys. Res. A* **547**, 50 (2005).
- <sup>18</sup>J. H. Park, E. Vescovo, H. J. Kim, C. Kwon, R. Ramesh, and T. Venkatesan, *Phys. Rev. Lett.* **81**, 1953 (1998).
- <sup>19</sup>H. Tanaka, J. Zhang, and T. Kawai, *Phys. Rev. Lett.* **88**, 027204 (2001).
- <sup>20</sup>M. Izumi, Y. Ogimoto, Y. Okimoto, T. Manako, P. Ahmet, K. Nakajima, T. Chikyow, M. Kawasaki, and Y. Tokura, *Phys. Rev. B* **64**, 064429 (2001).